Cyclic Testing of a Buckling Restrained Braced Frame with Unconstrained Gusset Connections

Jeffrey W. Berman[1] and Michel Bruneau[2]

Abstract: Buckling restrained braces are intended to yield in both axial tension and compression. The gusset plates connecting them to the adjacent beams and columns are thick and often stiffened to prevent buckling, and as a result increase the stiffness of the beam-to-column connection substantially. The increased stiffness of the beam-to-column connection negatively impacts the seismic performance of the system by: increasing the portion of the base shear force that is resisted by the frame relative to that resisted by the braces; increasing the maximum base shear force that the system is subjected to for a given earthquake motion; and transferring moment to the braces for which they were not designed. Further, failure of gusset welds partly due to the opening and closing of the beam-to-column joint has been observed in recent experiments. To mitigate these effects and increase the efficiency of buckling restrained braced frames, a novel connection where the gusset is only connected to the beam and is offset from the column face is proposed and tested in a three-story frame under quasistatic loading. The connection is shown to accommodate frame drifts as large as 3% and satisfy the buckling restrained brace performance requirements of the *2005 AISC Seismic Provisions for Steel Buildings*. Additionally, the portion of base shear force resisted by the braces relative to that resisted by the surrounding frame is shown to be consistent with design assumptions. This connection configuration could be particularly useful for retrofit of seismically deficient moment resisting frames.

DOI: 10.1061/(ASCE)ST.1943-541X.0000078

CE Database subject headings: Buckling; Bracing; Connections; Frames; Seismic effects; Experimentation; Cyclic tests.

Introduction

Buckling restrained braced frames (BRBFs) have been used as seismic and lateral load resisting systems for new and retrofit construction. Under large seismic motions, the full and stable hysteretic behavior of the buckling restrained braces (BRBs), which yield in both tension and compression, provides substantial energy dissipation and ductility. This behavior has been tested and well documented in several experimental studies (Wada et al. 1992; Iwata et al. 2000; Black et al. 2004; Lopez et al. 2004; among others) and there are clauses for the design of BRBFs in the *2005 AISC Seismic Provisions for Steel Buildings*, AISC 341 (AISC 2005a). Appendix T of AISC 341 requires that the satisfactory performance of BRBs and their connections to surrounding framing members (as part of an assembly) be demonstrated by testing.

Many past tests have documented instances of conformance to the AISC 341 requirements, the development of which is described in Sabelli (2004). However, when testing of complete BRBFs with gusset plate connections to the beams and columns has been performed, rather than tests involving only the BRB and gusset, cases of less-than-adequate performance have been observed (Tsai et al. 2003; Mahin et al. 2004; Tremblay et al. 2006; Christopulos et al. 2006; Tsai et al. 2006). These tests have highlighted the stiffening effect of the gusset on the connection and, in some cases, the limitations. Gusset performance is critical to the performance of BRBF systems and there are several ways in which gussets affect the system behavior:

1. The presence of the gusset at the beam-to-column connection creates a system that has a larger stiffness relative to a braced frame with assumed simple connections, which in turn decreases the period of vibration of the system and increases the seismic force demand.
2. The larger stiffness of the beam-to-column connection also results in a larger proportion of the base shear force being resisted through frame action rather than truss action, decreasing the effectiveness of the BRBs as described below.
3. Stiff gusset plates may transfer moment to the BRBs which reduces their cumulative inelastic axial deformation capacity.
4. Out-of-plane gusset buckling may occur as the angle between the column and the beam at the beam-to-column joint "closes" during frame sway, causing an out-of-plane moment on the BRB and the BRB connection to the gusset.
5. A low-cycle fatigue condition is created in the critical welds that connect the gusset to the beam and column. Tension stresses develop as the beam-to-column joint "opens" during frame sway and compression stresses develop as the joint closes. Such a low-cycle fatigue condition can lead to weld fracture.

The latter two points are of critical significance. Recent experimental work by Mahin et al. (2004) and Christopulos et al. (2006) showed damage to the gusset-to-beam-to-column connections, including fractures of the gusset welds and local buckling of the flanges and webs of the beams and columns along and near the gusset. The damage was observed at large drifts for braced frames (i.e., larger than 1.5%) but is nevertheless a concern for certain

[1]Assistant Professor, Dept. of Civil and Environmental Engineering, Univ. of Washington, Seattle, WA 98195-2700 (corresponding author). E-mail: jwberman@u.washington.edu

[2]Professor, Dept. of Civil, Structural, and Environmental Engineering, Univ. at Buffalo, Buffalo, NY 14260. E-mail: bruneau@buffalo.edu

Note. This manuscript was submitted on October 6, 2008; approved on May 10, 2009; published online on June 10, 2009. Discussion period open until May 1, 2010; separate discussions must be submitted for individual papers. This paper is part of the ***Journal of Structural Engineering***, Vol. 135, No. 12, December 1, 2009. ©ASCE, ISSN 0733-9445/2009/12-1499–1510/$25.00.

performance expectations of BRBFs. Fractures of the weld of the gusset to the beam resulted from stresses caused by the opening and closing of the angle between the column and beam at the beam-to-column connection. When opening, tensile stresses oriented approximately perpendicular to the BRB's longitudinal direction develop in the gusset and must be transferred through the gusset weld to the beam and column. When closing, the gusset plate is compressed and possibly buckled. If the gusset does buckle, the out-of-plane deformation would cause additional compression and tension stresses in the welds. Even if buckling does not occur the alternating cycles of tension and compression stresses can initiate fracture from low-cycle fatigue of the gusset weld.

To avoid these drawbacks an unconstrained configuration is proposed where the BRB gusset is connected to the beam and not to the column. A moment resisting beam-to-column connection is then employed to transfer the high shear force and increase beam stability. The proposed gusset connection is an alternative to the one developed and tested by Fahnestock et al. (2007) where the gusset is connected to both the beam and column but the moment is released from the beam via a rotationally flexible splice placed just outside the gusset region. Fahnestock et al. (2007) showed the system had good seismic performance and eliminated undesirable failure modes. While such a connection may be a practical alternative for new construction, it is difficult to employ in retrofit situations. The connection proposed here may be a practical alternative in retrofit scenarios and also has the benefit of maintaining the redundancy inherent in braced frames with moment-resisting beam-to-column connections.

The system described here was designed using the formalized structural fuse methodology (Vargas and Bruneau 2009a) and has been previously validated for seismic applications using dynamic earthquake simulation testing (Vargas and Bruneau 2009b). Those tests, whose primary goal was verification of the formalized structural fuse design methodology rather than an in-depth investigation of the behavior of the proposed BRB gusset connection, confirmed that the system met the performance objectives for the design seismic demands. However, the drift levels achieved during those tests were fairly small, albeit large enough to cause BRB yielding.

This paper describes the details of the design procedure and the results from quasistatic cyclic testing to failure of the BRBF using the proposed BRB gusset connection. The behavior of the connection is fully investigated and the behavior of the BRBs is separated from that of the surrounding moment resisting frame.

Structural Fuse Concept for BRB Design

To illustrate how minimizing the stiffness of the framing system around the BRBs helps to improve the efficiency of the BRBF system and keep the demands on the framing members low, a brief review of the structural fuse concept formulated by Vargas and Bruneau (2009a) is provided. This concept evolves from consideration of a frame with a generic structural fuse in Fig. 1(a) as represented by the three-spring model shown in Fig. 1(b), where K_f is the lateral stiffness of a frame (i.e., the moment-resisting frame), K_s and K_d are the lateral stiffnesses of the nonyielding segments of the BRB and the yielding segment of the BRB, respectively, m is the reactive mass, and C is the damping coefficient. The three spring model can be then be simplified to the model of Fig. 1(c), where the stiffness K_1 is

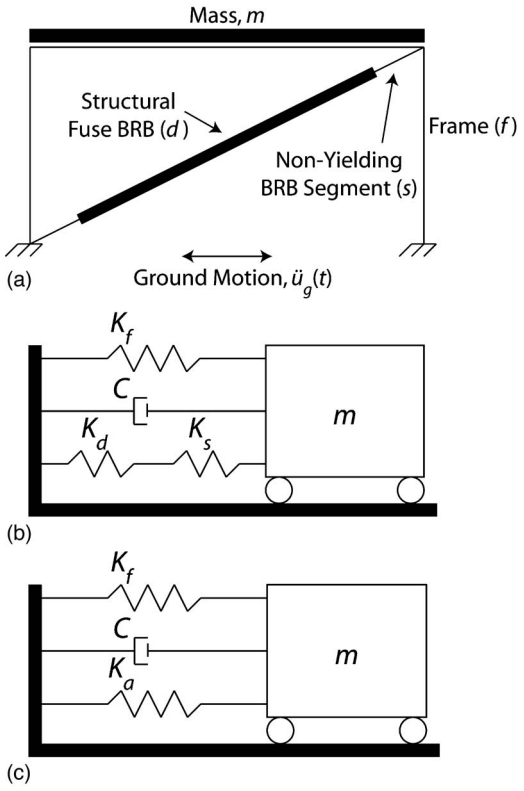

Fig. 1. (a) Frame system with generic structural fuse; (b) mass-spring representation; and (c) simplified mass-spring system

$$K_1 = K_f + K_a \tag{1}$$

and

$$K_a = \frac{K_s K_d}{K_s + K_d} \tag{2}$$

Considering elastic-perfectly plastic behavior for the frame and structural fuse, the system force-displacement curve shown in Fig. 2 would result, where Δ_{ya} is the displacement of the system when the structural fuse yields, Δ_{yf} is the displacement of the

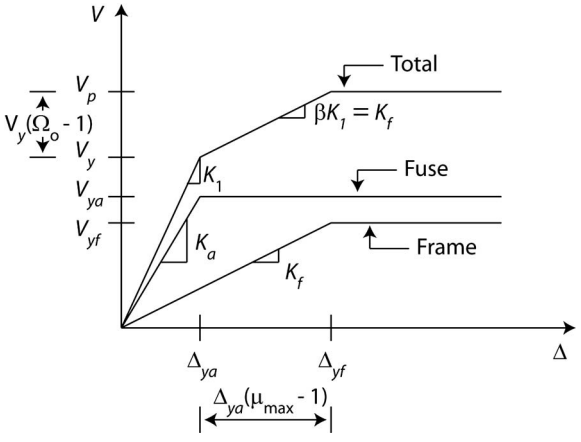

Fig. 2. Generalized pushover curve for system with a structural fuse

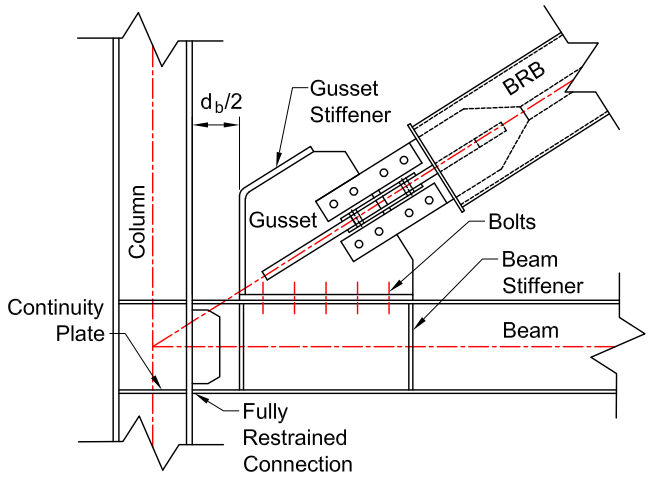

Fig. 3. Proposed gusset connection

system at frame yield, V_{yf} is the yield base shear force of the frame alone, V_{ya} is the yield base shear force of the structural fuse alone, V_y is the base shear force of the system when the structural fuse yields, and V_p is the base shear force of the system at frame yield. The objective of the structural fuse concept is to limit system response to less than Δ_{yf}, to allow self-centering of the undamaged frame upon removal and replacement of the yielded fuses (i.e., per a complete fuse analogy).

Using Fig. 2, the stiffness ratio β, maximum displacement ductility μ_{max}, and overstrength Ω_o, may be defined as

$$\beta = \frac{K_f}{K_1} \quad \mu_{max} = \frac{\Delta_{yf}}{\Delta_{ya}} \quad \Omega_o = \frac{V_p}{V_y} \tag{3}$$

where the displacement ductility is limited by frame yield. Vargas and Bruneau (2009a) performed a parametric study incorporating nonlinear time history analysis to develop a design tool for such a fuse system. However, the purpose of this study is to investigate the novel connection detail and in this case only the pushover curve is necessary to employ the structural fuse design methodology.

Considering Fig. 2, the most efficient use of a BRB as the structural fuse is when the difference between frame and brace yield displacements is maximized (i.e., when μ_{max} is maximized). Further, when BRB yielding occurs earlier in the loading history more energy is dissipated prior to frame yielding. Fig. 2 also assists in demonstrating the effect of stiffening the moment resisting frame by adding a large, thick, stiffened gusset of the type often used for BRBs. The increase in frame stiffness increases the total stiffness of the BRBF system, thus causing larger base shear force to develop. Once the BRBs yield, the larger base shear force owing to the stiffer frame must be carried by the frame, including the connections and foundations. In the context of seismic retrofit, this observation is significant because existing framing systems may not be able to resist the increased demand. Additionally, for new construction, this effect may not be accounted for in design of the frame and foundations, especially if the BRBF is analyzed neglecting frame action (i.e., as a truss). This frame stiffness increase is likely to be more significant in BRBFs relative to concentrically braced frames (CBFs) because the gusset plates in CBFs are typically designed to be somewhat flexible to allow the braces to buckle out-of-plane as desired.

BRB Connection Details

Fig. 3 shows a schematic of the proposed connection. As shown, the work point of the gusset connection is at the intersection of the beam and column centerlines (if not, it would require accounting for additional flexural demands on the beam, but that case is not considered here). Given that the location of beam plastic hinging is typically assumed to be at $d_b/2$ from the column face for moment resisting beam-to-column connections of the type considered here (Federal Emergency Management Agency 2000b), the gusset is offset a minimum distance of $d_b/2$ from the column face. As a result, the gusset edge may be at the expected location of a plastic hinge in the surrounding frame, when such a hinge forms at large drifts. For a gusset welded to the beam, beam plastic hinging would be expected to be constrained to the region between the column face and the gusset, and for a gusset bolted to the beam, hinging might be expected to spread around $d_b/2$. As discovered during testing and discussed in sections below, beam yielding was mostly limited to the region between the gusset edge and the column face despite the bolted gusset connection. Additionally, the increased stress state caused by the presence of the bolt holes did not initiate fracture in the beam flange.

As shown in Fig. 3, beam stiffeners should be provided where the gusset is connected to prevent web buckling and flange bending. In practice, these stiffeners could also be used for the required lateral bracing of the beam. The gusset is stiffened against buckling with an edge stiffener and a stiffener parallel to the longitudinal axis of the BRB, which is recommended whether a bolted connection or pin connection is used for the BRB. The compressive buckling strength of the gusset may be checked using Section of J4.4 of the *AISC Specifications for Structural Steel Buildings* (AISC 2005b) and free-edge buckling may be checked as per Astaneh-Asl (1998).

Regardless of whether the system is for new construction or retrofit, the beam-to-column connection should be moment resisting. An estimate of the necessary rotation capacity may be obtained from analysis and for new construction the choice of whether the connection should satisfy the requirements of special, intermediate, or ordinary moment frames could be made based on the required rotation capacity. Note that because the system has a first mode fundamental frequency of vibration near or above that of a braced frame, the drifts and rotation demands will be significantly lower than those associated with traditional moment resisting frames. In fact, Vargas and Bruneau (2009b) showed that it is possible to design this system such that there is 0 ductility demand on the beam-to-column connection for design earthquakes. For earthquakes exceeding the design level shaking, frame yielding will occur and ductile response of beam-to-column connections should be ensured. When connection ductility demands are large, moment resisting connections should satisfy the requirements for special moment resisting frames (SMRFs) or the requirements for ductile connections as given in FEMA 350 (Federal Emergency Management Agency 2000b). For frames using the proposed gusset connection, the maximum frame drift prior to failure will be governed by the rotational capacity of the beam-to-column connection, not the axial deformation of the BRB. Thus, the unconstrained gusset connection represents a tradeoff between gusset and beam-to-column connection performance limiting the system ductility. The former is a connection detail for which there is little experimental data available and the latter is a detail for which there is considerable data.

Per capacity design principles the gusset should be designed to resist the brace expected tension and compression strengths

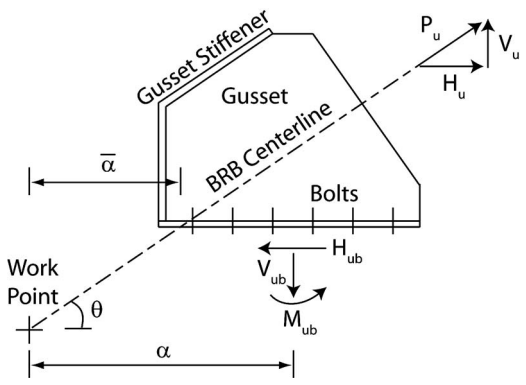

Fig. 4. Gusset free-body diagram

(AISC 2005a,b). Standard gusset plate limit state checks may be employed including yielding over the Whitmore section, net section fracture or tear-out, gusset buckling, and free-edge buckling. For design of the gusset-to-beam connection, the free-body diagram of the gusset shown in Fig. 4 may be used. Equilibrium considerations for the free-body diagram give the gusset-to-beam connection design loads as

$$H_{ub} = P_u \cos \theta \tag{4}$$

$$V_{ub} = P_u \sin \theta \tag{5}$$

$$M_{ub} = V_{ub}(\bar{\alpha} - \alpha) \tag{6}$$

where H_{ub}, V_{ub}, and M_{ub}=horizontal and vertical forces, and moment at the gusset-to-beam interface, respectively; P_u=expected BRB strength; and α and $\bar{\alpha}$=horizontal distances from the work point to where the projected brace centerline intersects the beam flange and to the center of resistance of the gusset-beam connection, respectively.

If the structural fuse methodology has been used to select framing member sizes and brace sizes, capacity design of the beams and columns should already be satisfied since the BRBs would be designed to yield at a drift that is much smaller than the yield drift of the moment resisting frame. Nonetheless, to ensure a fail-safe system, the designer should ensure that if the design drifts are exceeded, a desirable ultimate collapse mechanism is developed. That is also the case if a more traditional design approach is used rather than the formalized structural fuse methodology. The governing mechanism should consist of plastic hinging in the beams following BRB yielding and preceding other failure modes. Strong column-weak beam requirements should be satisfied to ensure that plastic hinges form in the beam rather than the columns. Furthermore, detailing the moment resisting connections to meet the requirements of an intermediate moment frame (IMF) or SMRF would ensure that the frame could reach a drift of 2 or 3%, or frame ductilities of approximately 2 or 3, respectively. The beam and beam-to-column connection should also have sufficient shear capacity since the shear force they transfer is larger than in traditional moment frames or brace-gusset connections. Consider Fig. 5, which shows a schematic of a beam from a frame with the proposed BRB gussets subjected to a drift large enough to cause both BRB yielding and plastic hinging of the beams (note that for BRBs in a chevron or inverted chevron configuration the situation would be similar). Equilibrium of the free-body diagram for the beam gives the following expressions for beam shear force demand, V_{bhr} and V_{bhl}, for the right and left ends of the beam, respectively

$$V_{\text{bhr}} = \frac{2M_{pb} + (P_{ui+1} + P_{ui})(s_h + d_c/2)\tan\theta}{L'} + P_{ui} \sin \theta \tag{7}$$

$$V_{\text{bhl}} = \frac{2M_{pb} + (P_{ui+1} + P_{ui})(s_h + d_c/2)\tan\theta}{L'} + P_{ui+1} \sin \theta \tag{8}$$

where M_{pb}=plastic moment capacity of the beam; P_{ui} and P_{ui+1} =expected strengths of the BRBs below and above the beam under consideration; s_h=distance from the column face to the beam plastic hinge; d_c=depth of the column; θ=inclination angle of the BRBs with respect to horizontal; and L'=distance between beam plastic hinges. In a retrofit situation, the beam-to-column connections may not be able to achieve ductility equal to that of an IMF, however, the shear strength of the connections should still be greater than required by Eqs. (7) and (8) to prevent brittle shear failure.

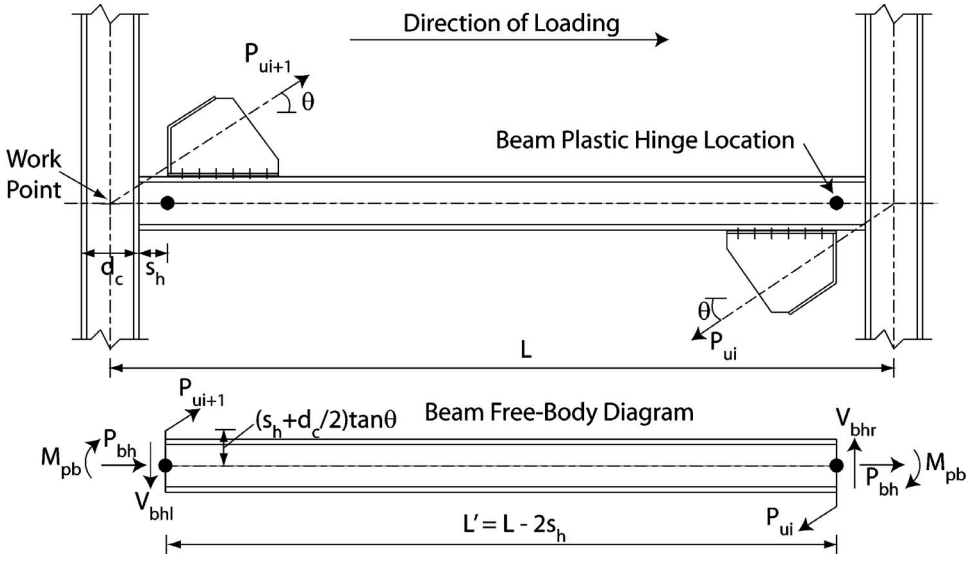

Fig. 5. Beam schematic and free-body diagram

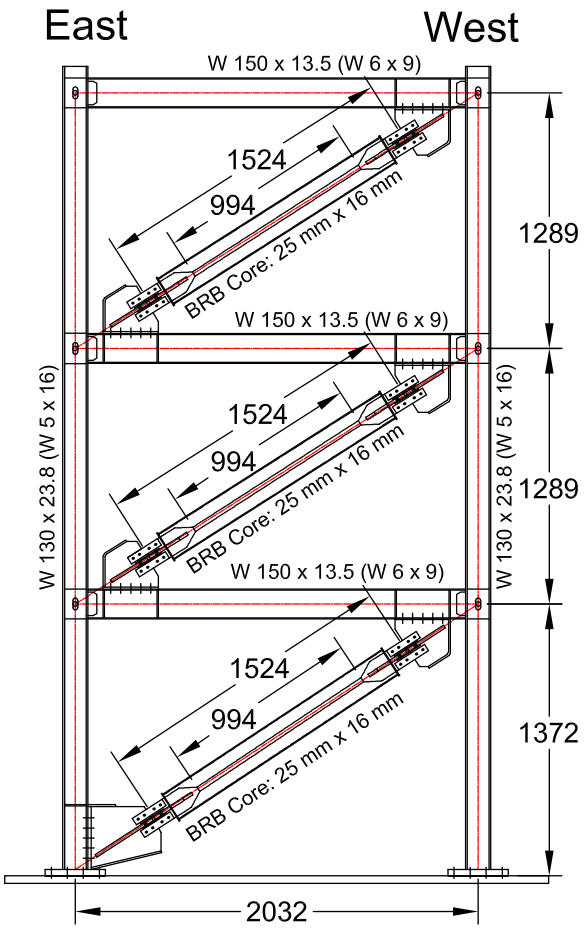

Fig. 6. Test specimen

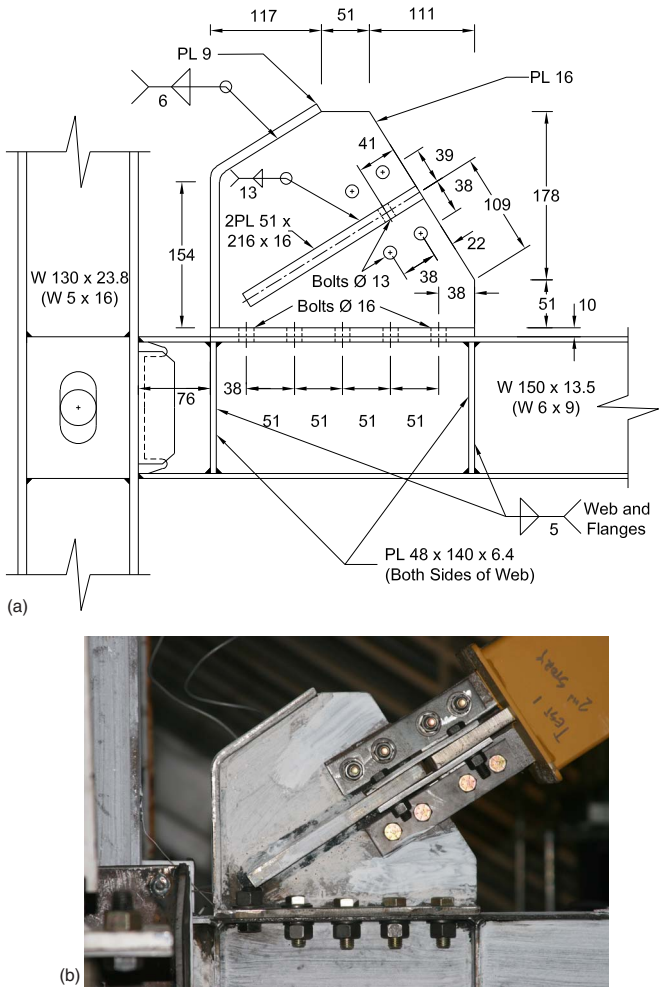

Fig. 7. BRB-to-beam connection detail (a) as designed; (b) after setup

Specimen Design

The specimen design is described in detail in Vargas and Bruneau (2009b), therefore, only a brief description is provided here. A prototype design was performed for the three-story SAC building (Federal Emergency Management Agency 2000a) for design ground shaking that was based on the performance capacity of the earthquake simulators in the Network for Earthquake Engineering Simulation node in the Structural Engineering and Earthquake Simulation Laboratory at the University at Buffalo (UB). The structural fuse methodology was employed for design of the prototype and the test specimen was designed from the prototype using a 1/3 length scale factor. As noted in Vargas and Bruneau (2009a,b) the analytical performance of the prototype and the results of dynamic testing of the specimen under design ground motions demonstrated that the design satisfied the performance objectives of the formalized structural fuse methodology, namely, that the frame remained elastic and the BRBs yielded, undergoing significant inelastic deformations. The 1/3 scale frame shown in Fig. 6 consisted of A992 Gr. 50 W150×13.5 (W6×9) beams and W130×23.8 (W5×16) columns, and SN400B (F_y =235 Mpa and F_u=400 Mpa) BRBs with a rectangular core cross-sectional area of 25×16 mm. Story heights were 1,340 mm for the first story and 1,289 mm for the second and third stories, and the bay width was 2,032 mm. Each end of each BRB was attached to the beams with the unconstrained gusset connections except the bottom of the first-story brace, which was connected directly to the column.

Typical BRB-to-beam and beam-to-column connections are shown in Fig. 7. Centerlines of the brace, beam, and column intersected at the center of the column panel zone and the BRB gusset was offset from the column face by a distance of 76 mm. The 16 mm thick gussets had 9.5-mm thick edge stiffeners as well as 16-mm stiffeners at the splice connection with the BRBs. The edge stiffeners were sized to be the same width as the beam flange and any remaining free-edge length satisfied the requirements of Astaneh-Asl (1998). Stiffeners were also provided for the beam on both sides of the web at the ends of gussets. The first-story BRB-to-column connection is shown in Fig. 8. As shown, the centerline of the BRB was aligned to intersect the centerline of the column at the top of the column's base plate and a stiffened gusset was bolted to the column flange.

Moment resisting beam-to-column connections were designed and a detail of the as built connection is shown in Fig. 9. Considering the 1/3 scale of the specimen, it was not possible to match all details of a connection from FEMA 350 (Federal Emergency Management Agency 2000b). Therefore, the connection was designed to be similar to a welded unreinforced flange-welded (WUF-W) web connection. Some key differences between the as-built connection and the WUF-W details from FEMA 350 are:

- The beam web was not welded to the column flange but rather only to the 6.4-mm shear tabs.
- There were two shear tabs, one on each side of the beam web,

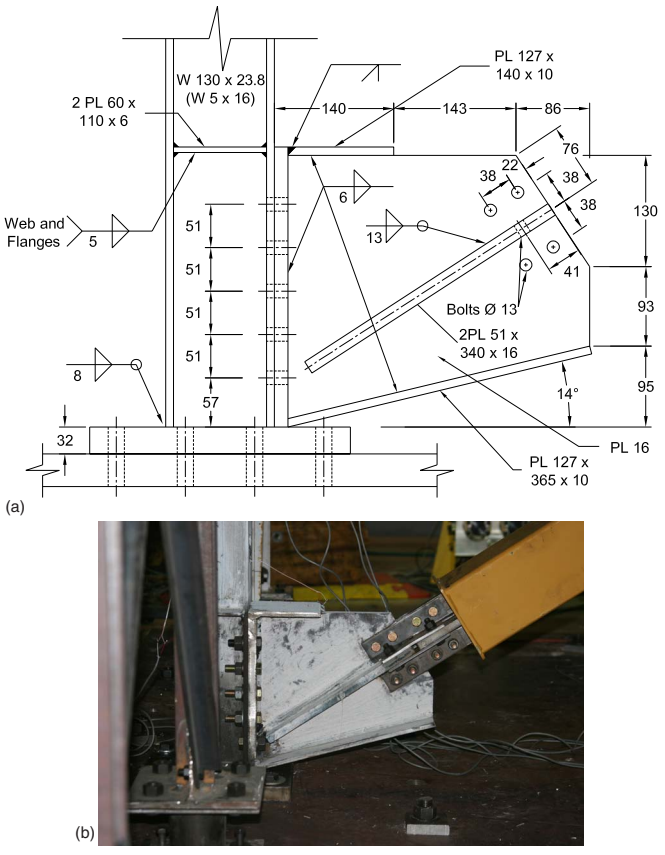

Fig. 8. BRB-to-column connection detail (a) as designed; (b) after setup (only on bottom story)

which were connected with complete joint penetration welds to the column flange and 4.7-mm fillet welds to the beam web.

- The radius for the weld access hole was 4.8 mm, and the center of the weld access hole was 9.5 mm from the inside of the adjacent flange, both of which are smaller than the minimum specified dimensions in FEMA 350.

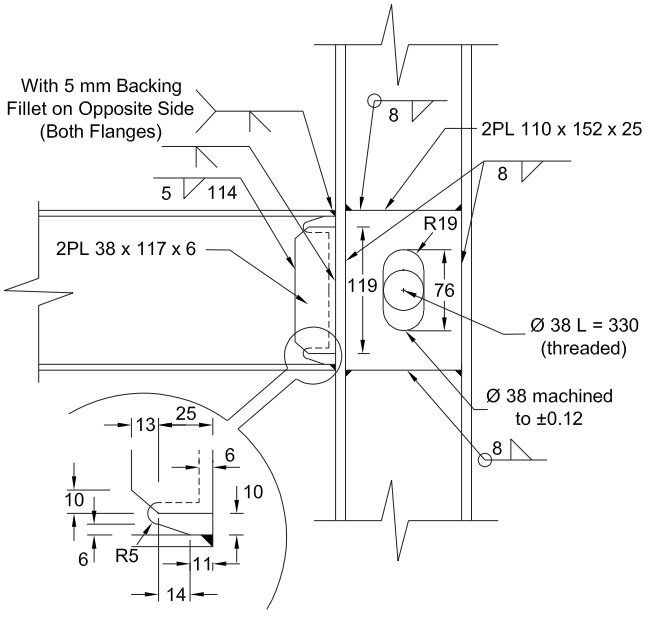

Fig. 9. Beam-to-column connection

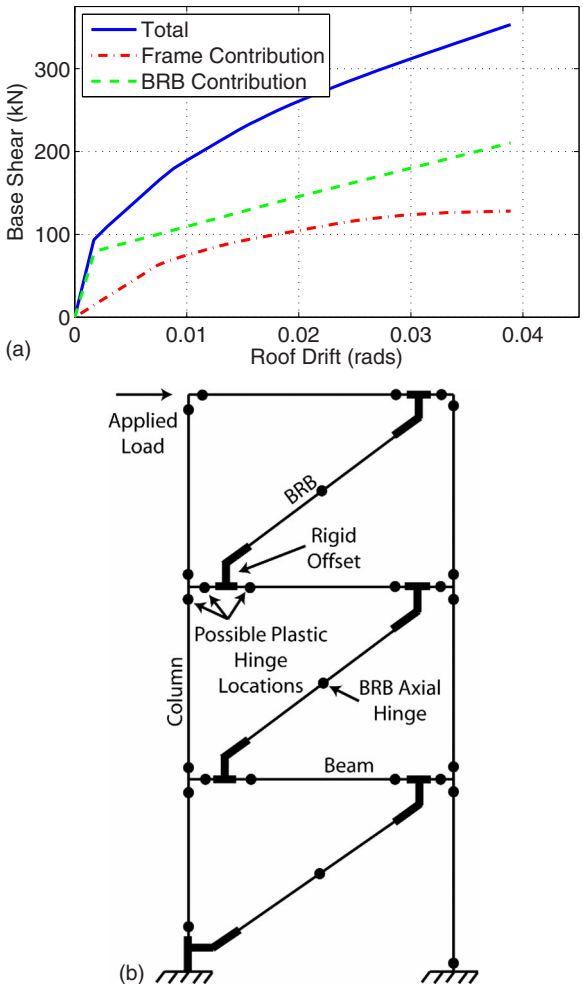

Fig. 10. Nonlinear static analysis for the test specimen (a) analytical pushover curve; (b) model schematic

- A hole was necessary in the middle of the column web panel zone for attachment of the reactive mass system [necessary for the earthquake simulation testing in Vargas and Bruneau (2009b) but used only for lateral bracing in the quasistatic testing described here]. The panel zone was then reinforced with a 25.4-mm doubler plate on each side of the column web.

The 1/3 scale specimen does not meet the qualification testing requirements for beam-to-column connections in AISC 341 (AISC 2005a,b), where the beam is required to have a depth of 90% of the prototype beam and a weight per foot of 75% of the prototype. Further, the detail changes above that were necessary to accomplish the required scale of the specimen may result in changes of the stress-strain history at critical fracture locations. Such changes could affect the low-cycle fatigue life of the connection. Therefore, near full-scale testing would be required prior to implementation of the proposed connection.

Nonlinear static analysis of a model of the experimental specimen was performed using SAP2000 (Computers and Structures Inc. 2004) and the results are shown in Fig. 10(a). The analysis considered a displacement pattern corresponding to a single actuator load at the top of the structure as discussed below. BRBs were modeled as elastic-plastic elements with only uniaxial yielding and 5% strain hardening based on the axial testing described in Vargas and Bruneau (2009b). Frame elements were also defined to have elastic-plastic flexural hinges with 1% strain hard-

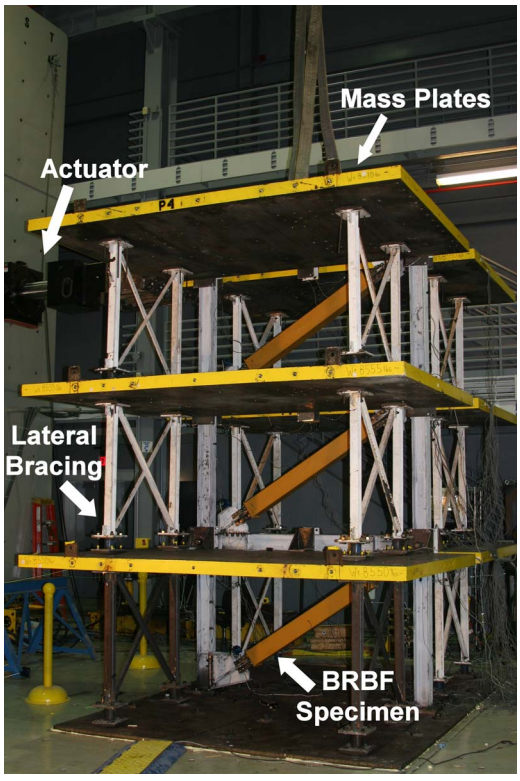

Fig. 11. Test setup

ening. No rotation limits for strength loss in the framing element hinges were assigned and all possible hinge locations in both the beams and the columns were considered. Rigid elements were used to represent the gussets and connected the brace end points to the centerline of the beam as shown in Fig. 10(b). The resulting pushover curves, shown for the bare frame, BRB's only, and frame with BRBs, indicate that the BRBs have been designed to yield at a roof drift of 0.17% while the frame will yield at a drift of 0.86% drift. For the prototype frame designed for the three-story SAC building, the roof drift at yield of the BRBs and frame were found to be 0.01 and 1%, respectively (Vargas and Bruneau 2009b). Thus, the analyses indicate that the prototype and the 1/3 scale experimental specimen exhibit reasonably similar global behavior. Additional details on the scaling of the specimen from the prototype design, and on the results of nonlinear response history analysis can be found in Vargas and Bruneau (2009b).

Experimental Setup and Loading

The specimen was attached to the strong floor of the laboratory at UB. Lateral support to the specimen was provided by the reactive mass frame used for the earthquake simulation testing. The reactive mass frame provides negligible resistance in the plane of the specimen, via the use of three-dimensional rockers at the top and bottom of each column at each story, while providing out-of-plane resistance through double-angle braces between the columns in that direction. The reactive mass frame has steel plates that are 90-mm thick, 2,000-mm wide, and 3,000-mm long separating the columns at each level and acting as beams. The connection of the plates to the specimen is achieved through 38-mm diameter high strength threaded bars that connect to vertically slotted holes in the webs of BRBF columns.

A large capacity static actuator was mounted to the adjacent strong wall and connected to the mass plates at the top story of the specimen as shown Fig. 11. The essentially rigid mass plates then transfer the actuator load to the tops of the columns of the BRBF. Loading was only applied at the top story of the specimen; therefore, the story shear force was equal at each level. The specimen was connected to a large steel floor plate at the column bases through connections capable of transferring the plastic moment capacity of the column. The floor plate was then pretensioned to the strong floor to prevent uplift of the specimen during testing.

The loading protocol used was based on Appendix T of AISC 341 (AISC 2005a,b) for qualifying cyclic testing of BRB test specimens, which specifies loading requirements in terms of BRB axial deformation. Roof drift was assumed to be proportional to BRB deformation and was used as the control quantity here because the frame was comprised of three BRB specimens. Prior to testing, the loading protocol was developed based on the results of the nonlinear static analysis described above. The brace deformation corresponding to the design story drift was assumed to be the brace deformation when the surrounding frame yields, in this case at 0.86% roof drift according to the nonlinear static analysis. This is a conservative upper bound on BRB deformation because the system was designed using the structural fuse methodology where the maximum drift for design ground motions is limited to the drift at which the frame surrounding the fuse elements begins to yield. Thus, 0.86% roof drift was substituted for brace deformation at design story drift in the loading protocol.

Table 1 gives values for the target percent roof drift and actual percent roof drift used as control for the quasistatic testing (the actual displacements applied were slightly different as a result of flexibility in the test setup). In Table 1, Δ is the roof displacement, δ is BRB axial deformation determined from displacement potentiometers that spanned the BRBs' length from gusset-to-gusset, Δ_y is roof displacement at yield of the first BRB (all three BRBs yield at very similar roof displacements), Δ_p is the inelastic roof drift computed as the total roof drift minus the base shear force divided by the frame's elastic stiffness, δ_y is yield axial deformation of the BRB (1.16 mm), and δ_p is the inelastic axial deformation of the BRB computed as the total BRB deformation minus the BRB axial force divided by the BRB's elastic stiffness. The brace deformation measurements include the deformation of the flared ends of the BRBs; however, their stiffness was 13 times larger than that of the BRB core making their contribution to BRB elongation negligible. After initial cycles, the loading protocol requires cycles be applied at 1.5 times the brace deformation at the design story drift until a cumulative BRB inelastic deformation of $200\delta_y$ is achieved. To approximate the cumulative BRB inelastic deformation prior to the test the roof drift was assumed to be proportional to BRB deformation, and the analytical model described above was used to estimate base force at the various drift levels. Table 1 shows the target and actual cumulative inelastic brace deformations, the latter determined using the BRB hysteretic curves described below. Through the beginning of Sequence 6 the loading protocol was consistent with that in Appendix T of the *ASIC Seismic Provisions*. At the end of Sequence 6 the system could be considered qualified per AISC (2005a,b), but only for the relatively small BRBs, beams, and columns used here. After Sequence 6, additional cycles at increasing drift levels were applied until failure of the specimen was observed.

Table 1. Loading Protocol and Brace Plastic Deformation Accumulation

		Target loading protocol				Actual loading protocol[a]						
							1st-story BRB		2nd-story BRB		3rd-story BRB	
Seq.	Number cycle	Drift %	Δ (mm)	Δ_p/Δ_y	$\Sigma(4\Delta_p/\Delta_y)$	Drift[b]%	δ_p/δ_y	$\Sigma(\delta_p/\delta_y)$	δ_p/δ_y	$\Sigma(\delta_p/\delta_y)$	δ_p/δ_y	$\Sigma(\delta_p/\delta_y)$
1	2	0.21	8.4	0.18	1.44	0.18	0	0	0	0	0	0
2	2	0.43	16.9	1.2	10.9	0.38	1.3	5.6	0.6	5.7	0.5	4.9
3	2	0.86	33.8	3.2	36.1	0.79	4.0	30.9	3.9	39.3	3.2	34.0
4	2	1.29	50.7	5.3	78.6	1.22	7.0	81.1	8.0	103.7	6.4	88.4
5	2	1.72	67.6	7.5	138.7	1.67	10.1	156.3	11.8	199.3	9.8	170.2
6[c]	24	1.29	50.7	5.3	528.5	1.23	6.9	767.9	7.6	955.1	6.4	826.1
7	2	2.00	78.4	9.0	720.4	1.89	12.1	860.4	15.0	1,068.2	11.9	922.1
8[d]	2	2.50	97.9	11.6	813.3	2.31	18.1	1,106.6	17.8	1,340.5	15.0	1,151.3
9	2	3.00	117.5	14.3	916.9	2.81	17.0	1,244.5	22.9	1,518.8	18.8	1,304.4
10	2	3.50	137.1	17.0	1052.9	3.29	18.0	1,389.6	25.5	1,717.4	20.5	1,471.6
11	2	4.00	156.7	19.7	1221.2	3.75	18.0	1,525.0	36.5	1,940.9	25.5	1,655.9

[a]Where differences in the peak positive and negative brace deformations were observed in a sequence, the maximum absolute value of those values is used in δ_p/δ_y. The summation includes the full unsymmetrical deformation pattern.

[b]There were minor differences between the maximum positive and negative drifts during a given cycle and the maximum absolute values for drift are given in the table.

[c]*AISC Seismic Provisions* Appendix t-test requirements were fulfilled during Sequence 6.

[d]Failure of the column base plate under the west column occurred during Cycle 2 of Sequence 8. Sequence 8 was restarted from the beginning following repair at the beginning of Sequence 8, resulting in four cycles at 2.31% drift.

Experimental Results

The base shear force versus roof drift hysteresis is shown in Fig. 12. Elastic specimen behavior was observed during the first two cycles although there was some friction in the system (this is shown as a small hysteretic area in the early cycles of Fig. 12). Yielding of the BRBs began in Cycles 3 and 4 (Sequence 2) at approximately 0.20%. At approximately 1% drift, during Cycles 7 and 8 of Sequence 4, frame yielding began with the beams at the first story, followed by the beams at the second story and then the beams at the third story. Recall the design intent, informed by nonlinear static analysis, was that there would be no yielding of frame members up to a drift of 0.86%. The BRBs, acting as fuses, yielded at a considerably lower drift of 0.17% and were responsible for all energy dissipation prior to yielding in the frame. The results indicate that this requirement was indeed satisfied as the BRBs began to yield at approximately 0.20% drift and had significant inelastic deformation prior to the onset of frame yielding.

After completing the testing requirements of Appendix T of AISC 341, the specimen was subjected to cycles at increasing

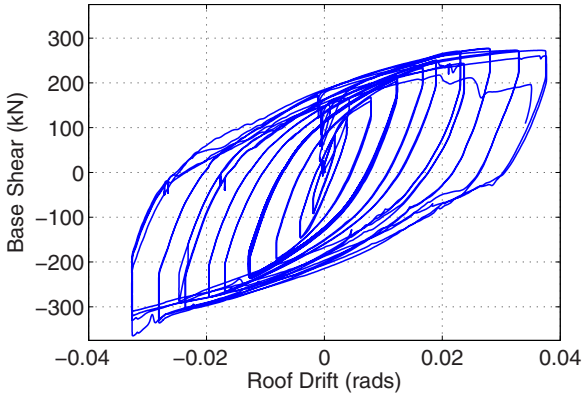

Fig. 12. Base shear force versus roof drift

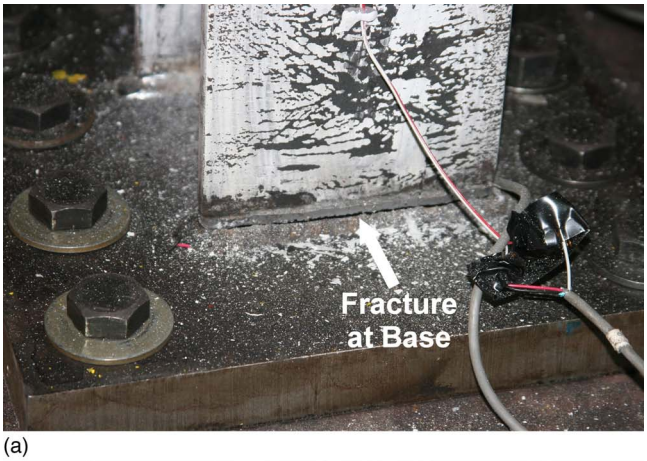

(a)

(b)

Fig. 13. (a) Fracture at west column base; (b) repaired west column base

Fig. 14. Beam-to-column connection fracture

drifts. During the cycles of Sequence 8 at approximately 2.3% frame drift, the weld connecting the west column to its base plate fractured as shown in Fig. 13(a). Note that the west column did not have the BRB connection at its base. The figure shows significant whitewash flaking indicating that the column had yielded extensively prior to the fracture. The connection was ground down and the column was rewelded to the base plate. Stiffeners were added to the base plate connections on both columns as shown in Fig. 13(b) to prevent subsequent fracture at the column base. The loading protocol was then continued with two additional cycles at 2.3% drift as shown in Table. 1.

In the cycles after the column base repair increasing plastic deformations of the BRBs and beams occurred. The specimen behaved in a ductile manner until the first floor beam-to-column connection at the west end of the beam fractured. Fig. 14 shows the fracture after testing and after the lateral bracing frames had been removed. The fracture occurred during the positive loading branch at 1.4% drift of what would have been the first cycle of Sequence 12, where the target roof drift was 4.5% (see Fig. 12 and Table 1). Following the fracture the specimen lost 30% of its strength. There was evidence of yielding, significant plastic deformation, and local buckling of the beam flanges at the connection.

Using strain gages that were placed in elastic regions of the beams and columns, the portions of the story shear force resisted by the frame and BRBs were separated. Fig. 15 shows those individual contributions for all three stories as backbone curves taken at the peaks of each cycle. The data for the first story shows the fracture of the weld at the west column base connection near 2.3% drift and the corresponding repair. As shown in Fig. 15 the BRBs resisted nearly 70% of the story shear force for the duration of the testing at all stories except the first story, where the percentage fell to slightly below 50% just prior to the fracture near the base plate of the west column. The figure also shows the clear linear behavior of the framing members well beyond the drift levels where the BRBs yield, consistent with the structural fuse concept. The first story had a somewhat larger stiffness relative to the upper two stories as indicated in Fig. 16, which shows the deformations of the west column at the positive peak of the final cycle of each sequence of loading. The first-story stiffness was expected to be larger because of the attachment of the gusset and BRB to the bottom of the east column as shown in Fig. 6. This connection is also the reason the portion of the first-story shear force carried by frame is larger than at the other two stories. The column deformation profile also shows that the relative deformations of the second and third story were similar; however, during the final cycles, the second story begins to absorb more of the total frame deformation.

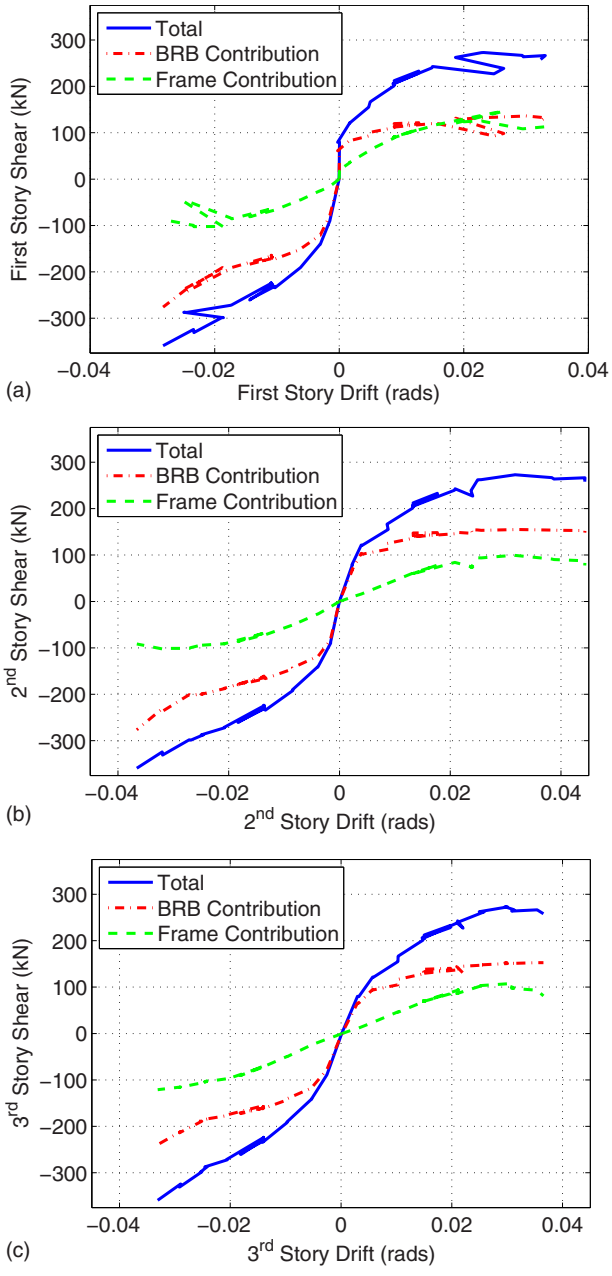

Fig. 15. Story shear force versus story drift backbone curves (a) first story; (b) second story; and (c) third story

Similar results to those above were obtained for energy dissipation, as shown in Fig. 17. The BRBs acted as a structural fuse and dissipated most of the hysteretic energy while the largest frame contribution was found to occur at the first story and the largest BRB contribution was found to occur at the second story.

Again using the strain gauge data to separate the response of various components, the BRB axial forces and the beam end moments were found. Fig. 18 shows BRB axial force P_{brb}, normalized by the yield axial force P_{ysc}, versus BRB axial deformation δ_{brb}, normalized by the yield deformation δ_{ybrb}. All BRBs had significant inelastic deformation and had stable hysteretic behavior. As expected, all BRBs had more strain hardening and developed larger strengths in compression than in tension due to

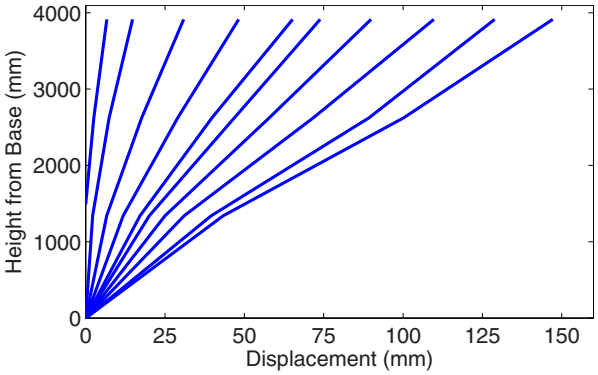

Fig. 16. Profile of west column at the maximum displacement of each sequence except Sequence 6

confinement of the lateral strains provided by the restraining material. Further, all BRBs showed increasing compressive stiffness near peak deformations in the final cycles caused by binding of the flared ends against the outer case of the BRBs. The first-story BRB appears to bind at a slightly lower deformation which may be attributed to the different gusset connection at the bottom of the first story. The BRBs at the second and third stories had the novel gusset connections at each end and were subjected to minimum rotations as the sections of the beams they were attached to remained approximately parallel. However, the first-story BRB was likely subjected to different rotations at each end because it was connected to two locations that did not stay approximately parallel (a column and a beam). The end rotations likely caused binding of the outer case of the BRB at a smaller axial deformation. Thus, another advantage of the novel gusset connection is that the in-plane rotation demands on the BRBs are reduced as they are connected to locations that remain approximately parallel in the deformed configuration. To achieve a similar behavior at the first story, the BRB could be connected to the foundation or a grade beam rather than the column.

Fig. 19 shows the moment at the west and east ends of the beams projected to the column faces, normalized by the beam plastic moment, versus the story drift. With the BRBs in this configuration, story drift may not correspond to connection rotation in the same way it does for a moment resisting frame. Considerable inelastic deformation of the first- and second-story beam-to-column connections is evident; however, the third-story connections had significantly less yielding. As noted, the west end of the first-story beam failed and that failure is apparent in the figures. Interestingly, it appears that a secondary load resisting mechanism must have developed after the failure since the moment at the east first-story beam-to-column connection continued to grow and the total base shear force was not immediately affected. Beam-to-column connection failure was the expected failure mode for the specimen and nonlinear static analysis results had indicated the first-floor connections were likely to fail first.

Fig. 20 compares a backbone curve of base shear force versus frame drift from the experimental results with those from nonlinear static analysis using SAP2000 (Computers and Structures Inc. 2004) which was described above. The analysis was repeated for both positive and negative loadings but the BRB properties were assumed to be equal for both compression and tension. Recall, the model assumptions included 5 and 1% strain hardening for the BRBs and frame member respectively. The model also included rigid offsets to represent the geometry, including the gussets, as shown in Fig. 10(b). From Fig. 20 it is clear the analysis results agree well with the experimental results. Thus relatively simple

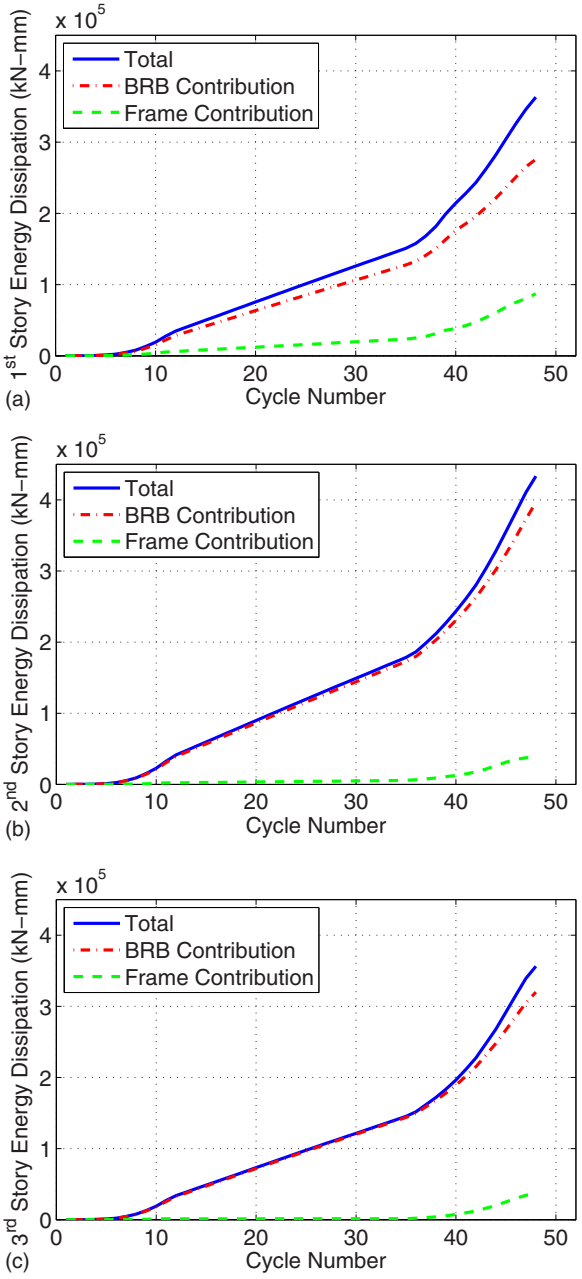

Fig. 17. Energy dissipation versus cycle number (a) first story; (b) second story; and (c) third story

nonlinear analysis static may be used to determine frame element forces for BRBF with the novel gusset connection developed here.

Conclusions and Recommendations

A new gusset plate connection for BRBs where they are connected only to the beam and not the column was designed and tested. The connection eliminates some of the problems that have been observed with BRB gusset connections in previous research including: the stiffening of the beam-to-column connection (resulting in larger frame stiffness and larger base shear forces), transfer of in-plane moment to the BRBs, out-of-plane buckling of the gusset, and gusset weld fracture due to the "opening" and "closing" of the beam-to-column connection during frame sway. As a trade off, it requires the use of a moment resisting beam-to-

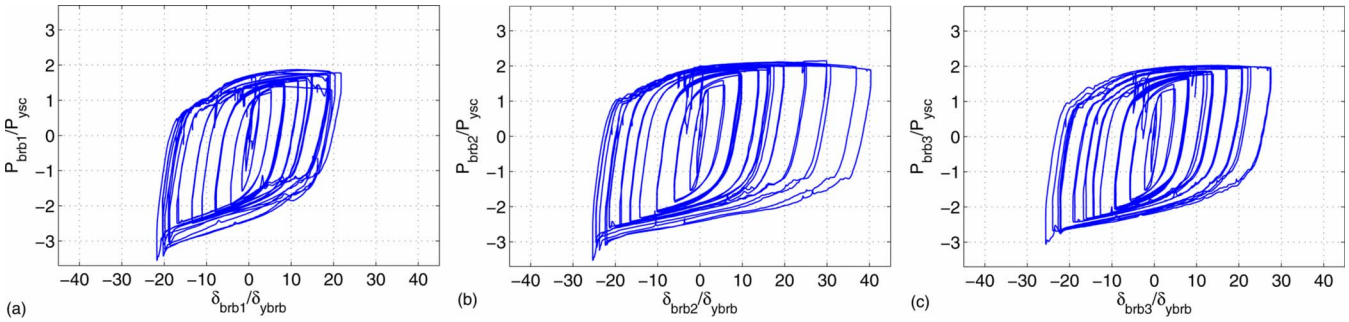

Fig. 18. BRB normalized axial force versus normalized axial deformation (a) first story; (b) second story; and (c) third story

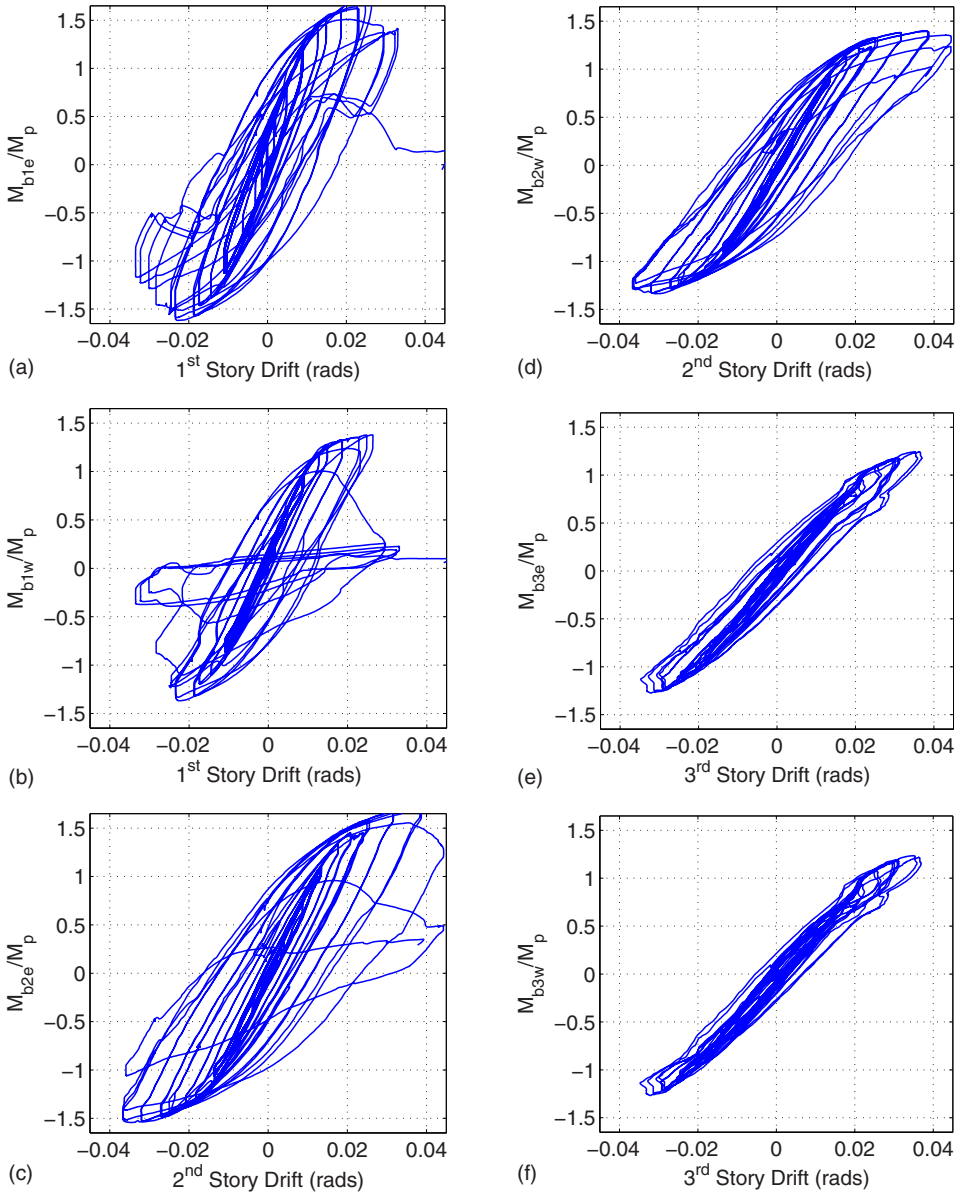

Fig. 19. BRB axial force versus axial deformation (a) first-story east; (b) first-story west; (c) second-story east; (d) second-story west; (e) third-story east; and (f) third-story west

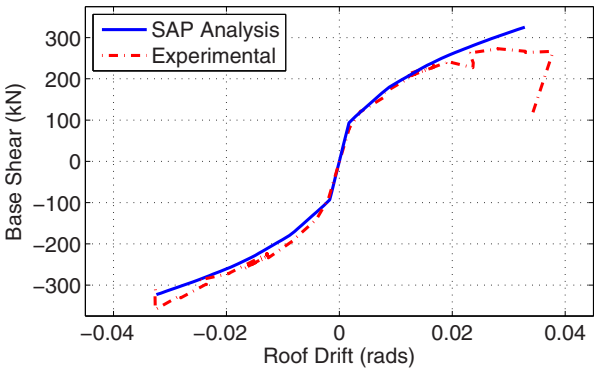

Fig. 20. Comparison of analysis and experimental base shear force versus roof drift backbone curves

column connection that will likely be the limiting factor in the system's ductility.

The three-story quasi-static BRBF test specimen with the novel gusset connection described here showed excellent ductility. BRB yielding occurred at 0.2% roof drift and reached an element ductility of almost 5 prior to the initiation of frame yielding at 1% roof drift. The system performed well throughout the required testing protocol of Appendix T of the AISC 341, meeting those performance goals. Additional testing to larger drifts followed the successful completion of the protocol. Ultimately the specimen reached a roof drift of 3.75% and a cumulative BRB inelastic deformation of over $1,500\delta_y$ when failure of the first-floor beam-to-column connection occurred and the testing was stopped. The system had been designed using the structural fuse methodology developed by others, where the design objective is to limit the maximum roof drift for design ground motions to less than the drift where yielding of the moment resisting frame occurs. This is done by ensuring the BRBs yield at a significantly lower drift levels and provide energy dissipation that controls peak frame drift. It was shown that the BRBs contributed significantly to the overall strength, stiffness, and energy dissipation capacity of the system and that the system performed as intended.

The BRBF specimen tested showed excellent ductility and proved the novel gusset connection to be a possible alternative to traditional BRB gusset plate configurations. However, the test was performed at 1/3 scale. Full scale testing should be performed to verify the performance of this type of connection prior to implementation. Of particular importance is the maximum ductility capacity, which is limited by the beam-to-column connection which in turn may be sensitive to modifications necessary for scaling. Further research would allow investigation of whether the peak roof drift of 3.75% can be achieved for a full-scale specimen, although that was well beyond the maximum allowed design roof drift of 0.86% necessary to satisfy the objectives of the structural fuse design methodology. If an alternative approach to the structural fuse design methodology is used in which yielding is expected at the beam-to-column connections, then ductility demands at the connections may approach the available ductility capacity.

Acknowledgments

This work was supported in part by the Earthquake Engineering Research Centers Program of the National Science Foundation under Award No. ECC-9701471 to the Multidisciplinary Center for Earthquake Engineering Research. However, any opinions, findings, conclusions, and recommendations presented in this paper are those of the authors and do not necessarily reflect the views of the sponsors.

References

AISC. (2005a). "Seismic provisions for structural steel buildings." *ANSI/AISC 341-05* and *ANSI/AISC 341s1-05*, Chicago.

AISC. (2005b). "Specifications for structural steel buildings." *ANSI/AISC 360-05*, Chicago.

Astaneh-Asl, A. (1998). "Seismic behavior and design of gusset plates." *Steel tips*, Structural Steel Educational Council, Moraga, Calif.

Black, C. J., Makris, N., and Aiken, I. D. (2004). "Component testing, seismic evaluation and characterization of buckling-restrained braces." *J. Struct. Eng.*, 130(6), 880–894.

Christopulos, A., Lehman, D., and Roeder, C. W. (2006). "Seismic performance of special concentrically braced frames with buckling restrained braces." *Proc., 8th National Conf. on Earthquake Engineering at the 100th Anniversary Earthquake Conf.*, EERI, Oakland, Calif.

Computers and Structures Inc. (2004). *Structural Analysis Program, SAP-2000NL Version 9.2.0: Integrated Finite Element Analysis and Design of Structures*, Computers and Structures Inc., Berkeley, Calif.

Fahnestock, L. A., Ricles, J. M., and Sause, R. (2007). "Experimental evaluation of a large-scale buckling-restrained braced frame." *J. Struct. Eng.*, 133(9), 1205–1214.

Federal Emergency Management Agency. (2000a). "State of the art report on systems performance of steel moment frames subject to earthquake ground shaking." *Rep. No. FEMA 355C*, FEMA, Washington, D.C.

Federal Emergency Management Agency. (2000b). "Steel moment frame buildings: Design criteria for new buildings." *Rep. No. FEMA 350*, FEMA, Washington, D.C.

Iwata, M., Kato, T., and Wada, A. (2000) "Buckling-restrained braces as hysteretic dampers." *Behaviour of steel structures in seismic areas: STESSA 2000*, Balkema, Rotterdam, The Netherlands, 33–38.

Lopez, W. A., Gwie, D. S., Lauck, T. W., and Saunders, C. W. (2004). "Structural design and experimental verification of a buckling-restrained braced frame system." *Eng. J.*, 4, 177–186.

Mahin, S., Uriz, P., Aiken, I., Field, C., and Ko, E. (2004). "Seismic performance of buckling restrained braced frame systems." *Proc., 13th World Conf. on Earthquake Engineering*, Int. Association of Earthquake Engineering (IAEE), Tokyo.

Sabelli, R. (2004). "Recommended provisions for buckling-restrained braced frames." *Eng. J.*, 4, 155–175.

Tremblay, R., Bolduc, P., Neville, R., and DeVall, R. (2006). "Seismic testing and performance of buckling-restrained bracing systems." *Can. J. Civ. Eng.*, 33(2), 183–206.

Tsai, K.-C., Hsiao, P.-C., Lin, S.-L., and Lin, K.-C. (2006). "Overview of the hybrid tests of a full scale 3-bay 3-story CFT/BRB frame." *Proc., 4th Int. Symp. on Steel Structures (ISSS '06)*, Korean Steel Structures Association (KSSC), Seoul, Korea, 73–84.

Tsai, K.-C., Weng, Y.-T., Lin, M.-L., Chen, C.-H., Lai, J.-W., and Hsiao, P.-C. (2003). "Pseudo dynamic tests of a full-scale CFT/BRB composite frame: Displacement based seismic design and response evaluations." *Proc., Int. Workshop on Steel and Concrete Composite Construction (IWSCCC-2003)*, National Center for Research in Earthquake Engineering, Taipei, Taiwan, 165–176.

Vargas, R., and Bruneau, M. (2009a). "Analytical response and design of buildings with metallic structural fuses: I." *J. Struct. Eng.*, 135(4), 386–393.

Vargas, R., and Bruneau, M. (2009b). "Experimental response of buildings designed with metallic structural fuses: II." *J. Struct. Eng.*, 135(4), 394–403.

Wada, A., Connor, J. J., Kawai, H., Iwata, M., and Watanabe, A. (1992). "Damage tolerant structures." *Proc., 5th U.S.-Japan Workshop on the Improvement of Structural Design and Construction Practices*, Applied Technology Council, Redwood City, Calif., 27–39.